

Originally published in *Proceedings of the Fifth International Workshop on Compressible Turbulent Mixing*, ed. R. Young, J. Glimm & B. Boston. ISBN 9810229100, World Scientific (1996).

Reproduced with the permission of the publisher.

Shock Tube Wall Boundary Layers Influence on the Measurement of Richtmyer-Meshkov Mixing Zone Thickness*

G. Jourdan and L. Houas

IUSTI - CNRS Umr 139
Université de Provence
Centre Saint Jérôme - Case 321
13397 Marseille CEDEX 20 - FRANCE

Abstract. A simultaneous tridirectional laser absorption technique for the shock induced Richtmyer-Meshkov mixing zone study is reported. The used method is an improvement of the CO_2 monodirectional laser absorption technique, using three detectors during the same run, instead of one, for the simultaneous thickness measurement of the mixing zone in the corners, near the walls and in the center of a square cross section shock tube. 2D front and rear shapes of the mixing zone and its volume are deduced from the experimental signals. Thickness evolution of the mixing zone is given in the cases when the shock wave passes from the heavy gas to the light one, from one gas to an other of close density and from the light gas to the heavy one. It is shown that the mixing zone is strongly deformed by the wall boundary layer when this last one becomes turbulent. On the other hand, it is found that, when the Atwood number tends to zero, we observe something like a limit regime and there is no more variation of the thickness of the mixing zone with the incident shock wave Mach number.

1 Introduction

When a shock wave crosses normally through the material interface between two fluids of different densities, the Richtmyer-Meshkov instability occurs, (Richtmyer [1], Meshkov [2]), leading to the birth and growth of a mixing zone between the two fluids. Since a quarter of century, shock tube experiments have been undertaken to simulate this phenomenon and the focus was made on the measurement of the thickness of the created turbulent mixing zone. Because of the perturbative influence of the shock tube wall

*This study was supported by the C.E.A. Centre d'Etudes de Vaujours-Moronvilliers, on contract No 304 843 / 00 D1.

boundary layers on the phenomenon under study, the classical integrated thickness measurement techniques provide ambiguous results. Up to this day, two laws of the temporal thickness evolution are suggested (Mikaelian [3], Youngs [4], Read [5], Zaitsev et al. [6] and Barenblatt [7]). The first is a linear evolution with the time and the second is proportional to a t^α power law, where α is lower than $\frac{2}{3}$. Which of these laws is the most representative of the phenomenon? Unfortunately, the answer to this question is not easy to give because, as it has been pointed out (Brouillette [8] and Houas et al. [9] and more recently Brouillette and Sturtevant [10]), it seems that the wall boundary layers stretched out the mixing zone to the shock tube walls and then favors, as time increases, the tending to the power law. Hence, a considerable effort is developed for carrying out new methods which allows more accurate thickness mixing zone determination and if possible, a quantitative estimation of the wall boundary layers effects. Thus, the aim of the present work is the undertaking of a new diagnostic technique based on the simultaneous tridirectional laser absorption of one of the two constituents of the mixing, which provides simultaneous informations within the mixing zone, in the center, that is far from the wall effects, near the walls and in the corners of the shock tube.

2 Experiments

2.1 Experimental set-up

Experiments are performed in a double diaphragm shock tube of about 9 meters total length. The test chamber is 8.5 cm by 8.5 cm square cross section and its length is about 115 cm downstream the second diaphragm for the measurements which concern the mixing zone before the coming back of the reflected shock. The shock tube end wall is movable and permits to position the interaction between the incident mixing zone and the first reflected shock at a selected abscissa. The test gases are CO_2 upstream, because of its spectroscopic properties, and Helium, Argon or Krypton downstream because they present no infrared absorption in the domain of our experiments, and also because they allow the study of the influence of the initial density configuration of the mixing zone: heavy/light for the CO_2/He case, close densities for the CO_2/Ar mixing and light/heavy for the CO_2/Kr one. They are initially separated by a thin plastic membrane (1.5 μm mylar) resting over a square grid of 5 \times 5 wires of diameter 0.2 mm and spacing 17 mm. Figure 1 presents the sketch of the general experimental set-up.

The simultaneous probing of different regions of the shock tube cross section is permitted by the using of ZnSe mirrors and beam splitters positioned along the incident laser beam optical path. The infrared detectors centered on 10.6 μm are cooled with liquid nitrogen and measure the absorption of the continuous wave CO_2 laser beam, when the mixing zone passes. Pressure gauges mounted flush at the walls are used to

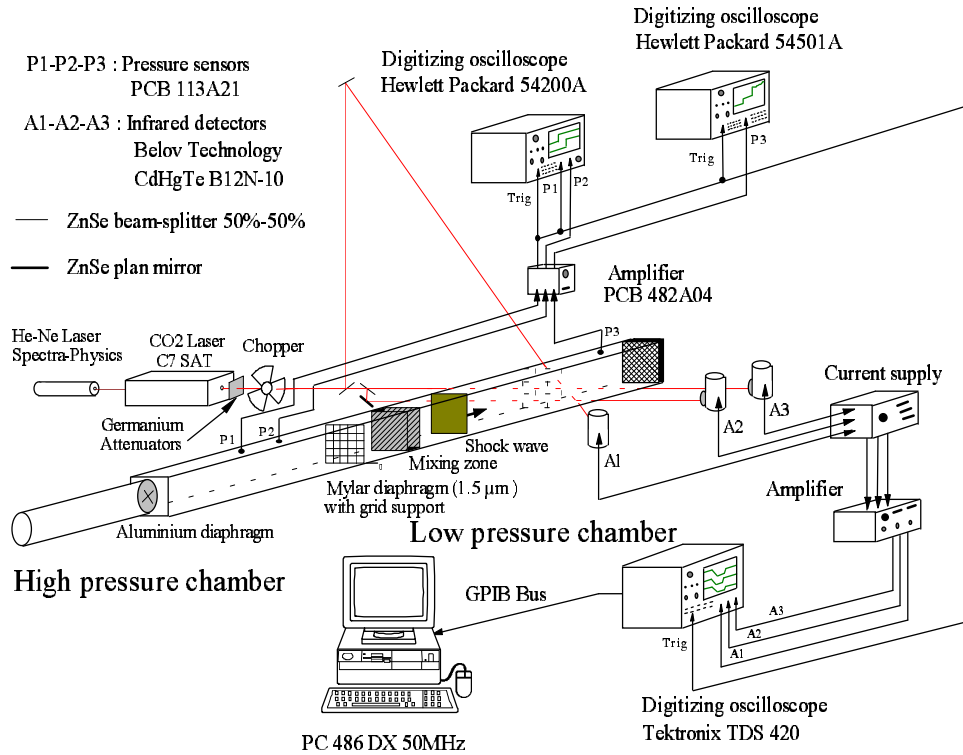


Figure 1: Experimental set-up.

record the passage of the shock waves.

2.2 Diagnostic method

The laser absorption principle of measurements has been previously described in the paper of Fortes et al. [11]. The absorption coefficient α depends on the temperature and the density of the absorbing medium (CO_2), at a determined frequency.

$$\alpha_\nu = f(T, \rho)$$

With two measurements at two different frequencies, the resolution of a system of two equations with two unknowns allows the determination of mean temperature and density profiles of the absorbing medium within the mixing zone. But in the present work, we have applied this infrared spectroscopic method for thickness determinations. Based on the paper of Wang [12], and considering the mixing zone to be non homogeneous, we have divided the test chamber cross section into 9 identical imaginary square regions

($\frac{85}{3} \times \frac{85}{3} mm^2$), where in each one, we consider the mixing zone to be homogeneous. As preliminary results (Jourdan et al. [13]) have shown that the mixing zone is invariant by rotation of 90° about the shock axis, we only probe one corner, one wall and the center of the shock tube, as shown in Figure 1. Figure 2 gives an example of simultaneous typical absorption signals, recorded during the same run, in the center, near one wall and in one corner of the shock tube. The different time passage of the mixing zone (Δt_{center} , Δt_{wall} and Δt_{corner}), and its velocity allow its thickness determination in the three characteristic regions of the shock tube. Therefore, the simultaneous using of three detectors permits to obtain a two dimensional visualization of the mixing zone shape, because we can estimate the absolute delay in time between the three absorption signals.

On the same figure, we observe that the plastic membrane particles do not perturb the mixing zone. Unfortunately, in some experiments these particles lie the mixing zone and prevent the processing of experimental data. Therefore, we use a metallic grid which allows a regular rupture of the membrane, and delays the membrane particles.

2.3 Initial conditions

Three couples of gases have been tested (CO_2/He , CO_2/Ar and CO_2/Kr) and absorption measurements have been realized for different incident Mach numbers in the CO_2 (2.4, 3.1, 4.5 and 5.3). But in this paper, focus is made on the results obtained with Mach number 3.1, which seems to correspond to the optimal conditions of our experimental diagnostic method. In fact, for low Mach numbers, there is a low signal to noise ratio, and for high Mach numbers, the temperature increases in such conditions so that the CO_2 is dissociated and the method is no more available. Four measurements have been realized, before the coming back of the reflected shock (164 mm, 335 mm, 550 mm and 775 mm). After compression, the quasi Taylorisation of the CO_2/Kr mixing zone does not permit a complete measurement because of the infinite time of the absorption signals, and thus, only CO_2/He and CO_2/Ar results are presented. One important thing to say is that for obtaining a measurement at a convenient abscissa, the shock tube wall end has been moved so that the interaction of the reflected shock with the incident mixing zone happens before the abscissa of the measurement (775 mm). Then, the total length of the experimental chamber was 880 mm for CO_2/He tests, 850 mm for CO_2/Ar and from 800 mm to 900 mm for CO_2/Kr but without successful results. The mixing zone velocities are 850 m/s, 640 m/s and 530 m/s for CO_2/He , CO_2/Ar and CO_2/Kr respectively before the interaction with the reflected shock and, 290 m/s and 55 m/s for CO_2/He and CO_2/Ar after compression (note that in CO_2/He experiments, He is polluted with 15 % of air). Before running the experiment, both parts of the experimental chamber are pumped to a vacuum of $4 \cdot 10^{-2}$ torr and then filled with the two test gases with the same initial pressure of about 1500 Pa in order to prevent

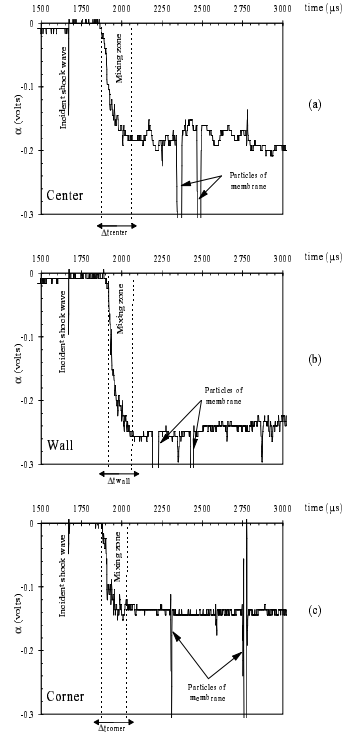


Figure 2: Example of simultaneous typical absorption signals recorded during the same run in the center (a), near one wall (b) and in one corner (c) of the shock tube.

from any large initial bulge.

3 Results and discussion

The accuracy on the thickness measurements is directly correlated with the reading of the time passage of the mixing zone (see Figure 2). It is estimated to be from about ± 1 mm for the lower velocity mixing zones to ± 4 mm for the higher cases.

Figure 3 shows the temporal thickness evolution measured in the center, near the walls and in the corners for each couple of gases. We have fitted all the experimental points with a t^α power law, with $0.4 \leq \alpha \leq 0.7$. As expected, we observe that, the thickness of the CO_2/He mixing zone is more important than the CO_2/Ar one. The CO_2/Kr case presents the smallest thickness. This result confirms that the mixing zone thickness increases with product $|At.\Delta U|$ ($|At.\Delta U|_{CO_2/He} = 620m/s$, $|At.\Delta U|_{CO_2/Ar} = 200m/s$ and $|At.\Delta U|_{CO_2/Kr} = 26m/s$). Furthermore, for each case, the thickness

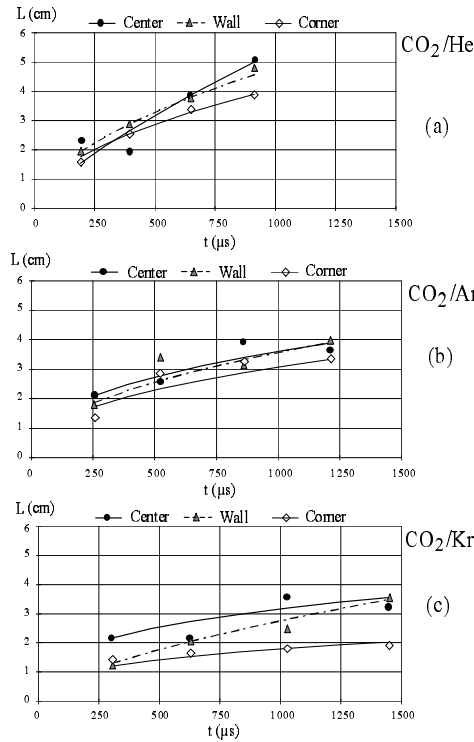


Figure 3: Temporal thickness evolutions of the CO_2/He (a), CO_2/Ar (b) and CO_2/Kr (c) mixing zones obtained with Mach number 3.1.

measured in the center is larger than the thickness measured near the walls, the corner value being the lower. The difference between the three measured thicknesses (center, wall, corner) is small for the CO_2/He mixing zone, more important for CO_2/Ar case, and large for the CO_2/Kr one.

Figure 4 represents the evolution of the volume of the mixing zone versus the time, for small (lower than 250 m/s), medium (between 250 and 600 m/s) and large (from 600 to 1400 m/s) $|At \cdot \Delta U|$ products. All the tests (3 couples of gases, 4 incident Mach number and 4 different abscissa) have been reported on this graphics. The results show that the volume increases with the time and the product $|At \cdot \Delta U|$.

In Figure 5a, we have plotted the 2D front and rear shapes of the mixing zone for Mach number 3.1, before and after it has been compressed by the reflected shock. Figure 5b represents a comparison of the mixing zone thickness in the center L_{center} , with its volume divided by the shock tube cross section $L^* = \frac{V}{S}$. If these quantities are close, one can conclude that the mixing zone is nearly a parallelepiped and the

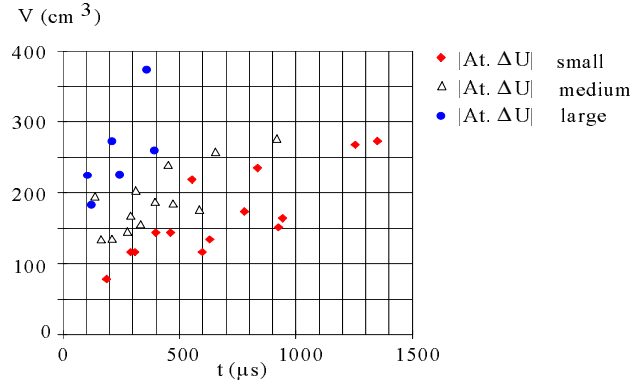


Figure 4: Evolution of the volume of the mixing zone versus the time for three different groups of $|At.\Delta U|$ product.

phenomenon under study is not too much perturbed by the wall effects. In the opposite case, that would mean that the thickness measurements are strongly dependent on this wall effect, which is not directly correlated to the Richtmyer-Meshkov instability itself. As we can see, the CO_2/He mixing zone is the least perturbed by the wall boundary layers. The 2D representations show, in this case, a mixing zone nearly a parallelepiped and the difference $\Delta(L_{center} - L^*)$ is small. For the other cases, CO_2/Ar and CO_2/Kr , the deformation of the mixing zone is clearly pointed out. Moreover, margin between L_{center} and L^* increases for the CO_2/Ar mixing zone and is maximum for the CO_2/Kr one. These observations have to be correlated with the hydrodynamic state of the wall boundary layer behind the incident shock wave in the monatomic gas. Calculations, based on the work of Mirels [14], have shown that the mixing zone propagates in a laminar boundary layer for CO_2/He case, transitional for CO_2/Ar and turbulent for CO_2/Kr one. From an other hand, thicknesses measured after compression (60 μs and 100 μs later for the CO_2/He and CO_2/Ar cases respectively) show that the factor of compression is more important for the CO_2/Ar mixing zone (75 %) than the CO_2/He one (50 %). We attribute this to the fact that in the first case, we are very near the Taylorisation and then the shock-interface interaction is more intense. Concerning this figure, a last point has to be related. As each experimental 2D visualization of the mixing zone is obtained from one run, the fact that the CO_2/He and CO_2/Ar mixing zones are bulged in the same direction, before and after the compression by the reflected shock, is coincidental.

Finally, we have plotted on Figure 6 the evolution of the thicknesses of the mixing zone, L_{center} and L^* , obtained for the different Mach numbers, and the three couples

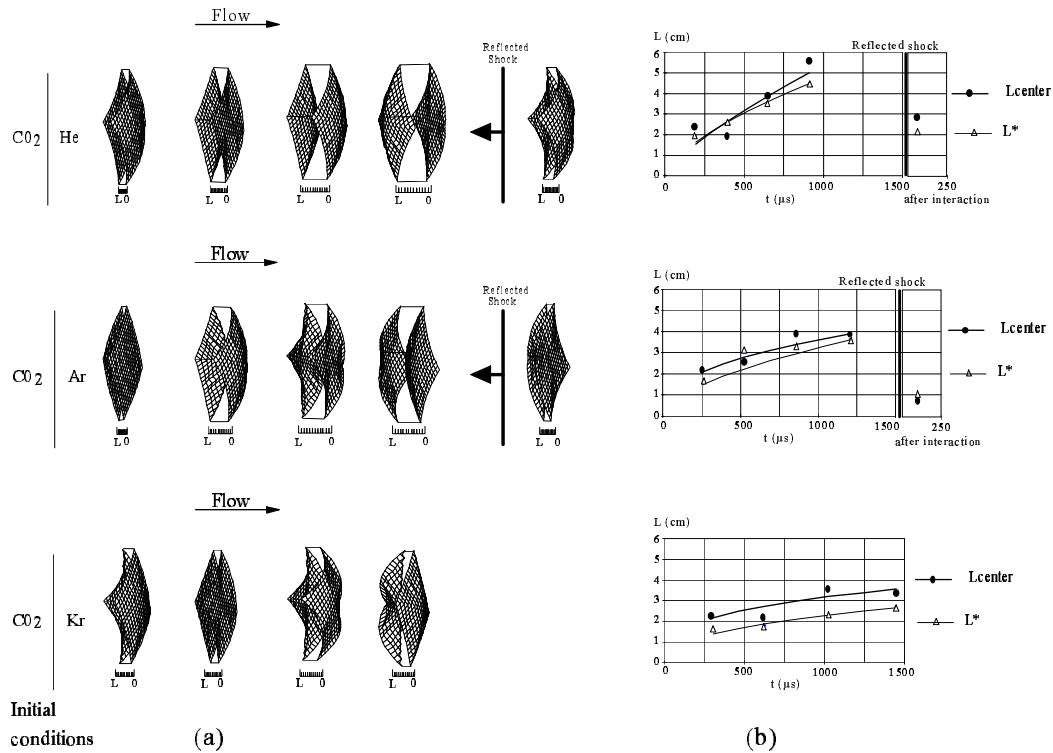


Figure 5: 2D front and rear shapes of the mixing zone for Mach number 3.1 (a) and comparison of L_{center} with $L^* = \frac{V}{S}$ (b).

of test gases. For the CO_2/He mixing zone, we observe that both the thickness and $\Delta(L_{center} - L^*)$ increases with the incident Mach number. For the CO_2/Ar case, if the thickness increases also with the Mach number, the evolution of $\Delta(L_{center} - L^*)$ is no more coherent. In the last case, CO_2/Kr , results are completely unexpected, since the variations of the thickness and $\Delta(L_{center} - L^*)$ do not follow a logical evolution. Moreover, if the different cases are clearly distinct for the CO_2/He mixing zone, the margin between the lower Mach number and the higher one diminishes for CO_2/Ar and CO_2/Kr cases. Furthermore, the ratio of the product $|At \cdot \Delta U|$ for higher Mach number and lower one, are about 2, 5 and 10 for CO_2/He , CO_2/Ar and CO_2/Kr cases respectively. We have found no explication for these paradoxical results, but it seems that we tend to a limit regime for the case where the Atwood number is close to zero, and we find no more variation of the thickness of the mixing zone with the incident Mach number of the shock wave.

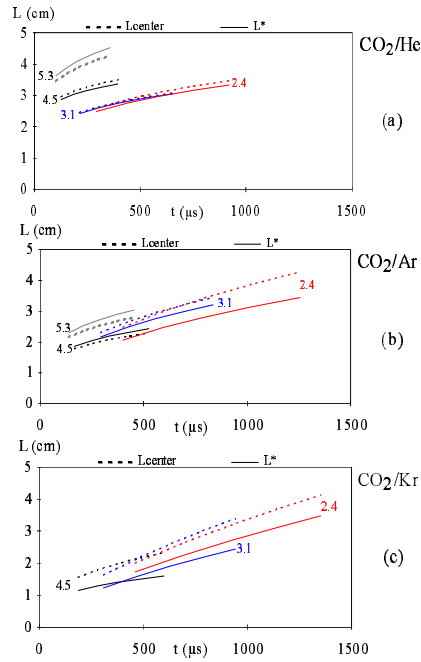


Figure 6: Evolution of the thicknesses, L_{center} and L^* , of the CO_2/He (a), CO_2/Ar (b) and CO_2/Kr (c) mixing zones obtained for the different Mach numbers.

4 Conclusion

Thickness measurements of a gaseous mixing zone originated from the Richtmyer-Meshkov instability have been undertaken for the cases when the shock wave passes from the heavy gas to the light one, from one gas to an other of close density and from the light gas to the heavy one. We have shown that the laminar boundary layer behind the shock wave slowly deforms the mixing zone but the deformation becomes quickly important when the boundary layer is turbulent. This result is confirmed by the 2D visualizations of the mixing zone obtained from the experiments.

Finally, it seems that the influence of the incident shock wave Mach number in the first gas on the thickness of the mixing zone decreases when the Atwood number tends to zero.

References

[1] Richtmyer RD, (1960), Taylor instability in shock acceleration of compressible fluids. Communication on pure and applied mathematics 13,297-319

- [2] Meshkov EE, (1970), Instability of a shock wave accelerated interface between two gases. NASA TT F-13, 074.
- [3] Mikaelian KO, (1990), Turbulent energy at accelerating and shocked interfaces. *Physics of Fluids* 2, 592-598.
- [4] Youngs DL, (1984), Numerical simulation of turbulent mixing by Rayleigh-Taylor instability. *Physica* 12D, 32-44.
- [5] Read KI, (1984) Experimental investigation of turbulent mixing by Rayleigh-Taylor instability. *Physica* 12D, 45-48.
- [6] Zaitsev SG., Lazareva EV., Chernukha VV and Belyaev VM, (1985), Intensification of mixing at the interface between media of different densities upon the passage of a shock wave through it. *Sov. Phys. Dokl.* 30,579-581.
- [7] Barenblatt GI (1983), Self-similar turbulence propagation from an instantaneous plane source. *Non linear dynamics and turbulence*, Barenblatt GI, Loos G and Joseph DD, eds Pitman, Boston, 48.
- [8] Brouillette M (1989), On the interaction of shock waves with contact surfaces between gases of different densities. Ph. D. Thesis, California Institute of Technology.
- [9] Houas L, Chemouni I, Touat A and Brun R (1991), Experimental investigation of Richtmyer-Meshkov induced turbulent mixing over long distances. *Proceedings of 3th International Workshop on the Physics of Compressible Turbulent Mixing*, Royaumont, France, 127-136, Eds CEA-DAM.
- [10] Brouillette M and Sturtevant B (1993), Experiments on the Richtmyer-Meshkov instability: Small-scale perturbations on a plane interface. *Physics of Fluids* A5, 4, 916-930.
- [11] Fortes J, Ramdani A and Houas L, (1994), CO_2 laser absorption measurements of temperature and density in shock induced Richtmyer-Meshkov mixing zone. *Physical Review E*, 50, 4, 3041-3049.
- [12] Wang JT, (1976), Laser absorption methods for simultaneous determination of temperature and species concentration through a cross section of radiating flow. *Applied Optics*, 15, 13, 768-773.
- [13] Jourdan G, Touat A, Chemouni I and Houas L (1994), Multi-directional laser absorption technique for simultaneous determination of temperature and concentration within a shocked gaseous interface, *Proceedings of the 7th International Symposium on Application of Laser Techniques to Fluids Mechanics*, Lisbon, Portugal, Vol 1, 20.3.1.
- [14] Mirels H, (1984), Turbulent boundary layer behind constant velocity shock including wall blowing effects. *AIAA J* 22, 1042-1047.